High spin structure in odd-proton nuclei ^{129,131}Pr

P. K. Weng, P. F. Hua, S. G. Li, S. X. Wen, L. H. Zhu, L. K. Zhang,
G. J. Yuan, G. S. Li, P. S. Yu, and C. X. Yang
China Institute of Atomic Energy, P.O. Box 275(10), Beijing, China

X. F. Sun, Y. X. Guo, and X. G. Lei
Institute of Modern Physics, Academia Sinica, Lanzhou, China
(Received 17 September 1991)

High spin states in ^{129}Pr and ^{131}Pr have been investigated using in-beam γ-ray spectroscopy techniques. The yrast band of ^{129}Pr based on the $h_{11/2}$ $\frac{3}{2}^-[541]$ proton configuration was observed from $\frac{11}{2}^-$ up to $\frac{43}{2}^-$. The band based on the same configuration and two positive-parity side bands based on the $g_{7/2}$ $\frac{5}{2}^+[413]$ proton configuration, were observed in ^{131}Pr. The delayed yrast band crossing of ^{129}Pr at $\hbar\omega_c = 0.37$ MeV is interpreted as being due to the alignment of the second and third $h_{11/2}$ protons. The band crossing at $\hbar\omega_c = 0.26$ MeV, with a gain in alignment of about $8\hbar$, based on the $g_{7/2}$ $\frac{5}{2}^+[413]$ configuration in ^{131}Pr was attributed to the alignment of two $h_{11/2}$ protons. The systematics of the proton alignments in a series of Pr isotopes is discussed.

PACS number(s): 23.20.Lv, 21.10.Re, 27.60.+j

I. INTRODUCTION

Light rare-earth nuclei in the mass $A = 130$ region are predicted to be soft with respect to γ deformation. Nuclear shape changes may occur when quasiparticles align [1]. The Fermi level of the protons in ^{129,131}Pr lies near the bottom of the $h_{11/2}$ shell, while that of the neutrons lies in the middle of the $h_{11/2}$ shell. Thus, it has been suggested that the alignment of a pair of $h_{11/2}$ protons would result in a drive to a collectively rotating prolate shape (γ about 0°, Lund convention [2]), whereas the alignment of a pair of $h_{11/2}$ neutrons would have an opposite effect, resulting in a drive toward a collectively rotating oblate shape (γ about $-60°$). In the even Ce isotopes [3–5], a band crossing caused by the alignment of a pair of $h_{11/2}$ protons has been observed to occur at the same rotational frequency in both the yrast band and two sidebands. For the odd-proton nuclei Pr, the yrast band is based on a decoupled $h_{11/2}$ proton. As a result, the band crossing of this $h_{11/2}$ proton pair is blocked. But in nonyrast sidebands, the $h_{11/2}$ proton pair alignment can still occur if other proton (or neutron) configurations are included. The crossing frequencies for the sidebands are of particular interest because of the influence that the odd-proton nuclei might have on the nuclear shape and on the proton pairing gap. Comparing the alignment crossing frequency in odd-proton nuclei with even-even neighboring nuclei may provide valuable information on the reduction of the proton pairing gap. The band crossings of $h_{11/2}$ proton pairs in the yrast and sidebands have been observed in ^{133,135}Pr nuclei [6,7]. In order to continue the systematic study of these band crossing features, the band structure of the odd-proton nuclei ^{129,131}Pr was investigated in detail in the present work.

The high spin structure of the nucleus ^{131}Pr has been studied by Godfrey *et al.* [8] using the ^{98}Mo(^{37}Cl,4n) reaction. These authors have established the yrast states from ($\frac{11}{2}^-$) to ($\frac{47}{2}^-$) and a sideband consisting of a cascade of six γ-ray transitions, which feeds into the yrast state at ($\frac{19}{2}^-$). For the ^{129}Pr nucleus, no level scheme has been reported before this work.

II. EXPERIMENTAL PROCEDURE

The odd-proton nuclei ^{129,131}Pr have been studied using in-beam γ-ray spectroscopy techniques. High spin states in these nuclei were populated following the ^{107}Ag(^{28}Si,2p2n)^{131}Pr and ^{107}Ag(^{28}Si,2p4n)^{129}Pr reactions at a beam energy of 128 MeV. In order to identify the different species produced at this beam energy, cross bombardment using the ^{116}Sn(^{9}F,4n)^{131}Pr reaction at a beam energy 93 MeV has also been done. The ^{28}Si and ^{19}F beams were provided by the Tandem HI-13 accelerator of the China Institute of Atomic Energy, Beijing. For both reactions, γ single spectra and γ-γ coincidence spectra were measured. The γ-ray angular distribution measurement was performed only with the Si induced reaction. One HPGe detector was positioned successively at each of five angles with respect to the beam axis: 15°, 35°, 55°, 70°, and 90°. The distance between the detector and target was approximately 20 cm. A second HPGe detector located at $-90°$ served as a monitor. The ^{107}Ag target (with 99% enrichment) of 2.0 mg/cm^2 thickness rolled onto a 10 mg/cm^2 natural lead backing was used for the Si induced reaction and a 3.0 mg/cm^2 ^{116}Sn target (with enrichment 98%) rolled onto a 15 mg/cm^2 natural lead backing was used for the ^{19}F induced reaction. The excitation function for the various ^{107}Ag(^{28}Si,x) reactions was measured at beam energies of 124, 128, and 138 MeV. ^{152}Eu and ^{60}Co sources were used for energy and efficiency calibrations. The experimental facility and the associated electronics which include a BGO Compton-

suppressed HPGe detector array have been described in detail elsewhere [9]. In this experiment, an array of five BGO-suppressed Ge detectors was used in the γ-γ coincidence measurement. The energy resolution of the detectors varied from 1.9 to 2.1 keV for the 1.332 MeV γ rays of ^{60}Co. The data were analyzed off-line on a VAX-11/780 computer by establishing two-dimensional $4k \times 4k$ coincidence matrices. Background subtracted gated spectra were generated from the matrices in order to construct the level scheme of ^{129,131}Pr. The total number of γ-γ coincidence events was about 4×10^7.

III. RESULTS

The level schemes of ^{131}Pr and ^{129}Pr obtained from the present study are presented in Figs. 1(a) and 1(b). The ordering of γ rays is determined on the basis of coincidence relationships and of γ-ray intensities. Some of the transitions could only be seen when several gated spectra within the same band were added. Some examples of gated background subtracted γ-γ coincidence spectra in ^{129}Pr and ^{131}Pr are shown in Fig. 2. The CASCADE calculations of the cross sections for the reaction ^{107}Ag(^{28}Si,x) at a beam energy of 128 MeV indicate that relative populations for the various channels are as follows: ^{131}Pr, 35%; ^{129}Pr, 3.1%; ^{132}Pr and ^{132}Nd, 15% each; ^{128,129}Ce, 10% and 12.5%, respectively; and other nuclei about 10%. As a large number of transitions from different reactions will appear in the γ-ray spectra, many γ-ray transitions in ^{129}Pr or ^{131}Pr are contaminated by other transitions. In order to identify some weak γ rays in ^{129}Pr or ^{131}Pr, it was necessary to discriminate against the γ rays from other nuclei in both the ^{107}Ag(^{28}Si,x) and the ^{116}Sn(^{19}F,x) reactions rather carefully.

Information on transition multipolarities was obtained from the measurement of γ-ray angular distributions. The formula

$$W(\theta) = A_0 + A_2 P_2(\theta) + A_4 P_4(\theta)$$
$$= A_0[1 + A_{22} P_2(\theta) + A_{44} P_4(\theta)] \quad (1)$$

(where $A_{22} = A_2/A_0$, $A_{44} = A_4/A_0$) was fitted to the observed γ-ray intensity function $W(\theta)$. Here, θ is the angle of the detector measured with respect to the beam axis, A_0, A_2, and A_4 are adjustable parameters, while P_2 and P_4 are Legendre polynomials. For some γ-ray transitions in ^{129,131}Pr, the extracted values of A_{22}, A_{44} together with their energies, intensities, spin, and parity assignments are listed in Table I. These intensity values have been corrected for the efficiency of the Ge detectors and normalized to the $\frac{15}{2}^- \rightarrow \frac{11}{2}^-$ transitions at the bottom of the yrast bands in the two nuclei ^{129}Pr and ^{131}Pr, respectively. The spin and parity assignments of the lower members in the yrast bands of ^{131}Pr and ^{129}Pr have been made on the basis of the angular distribution data, with the help of the systematics on Pr isotopes in the framework of the Nilsson schemes. The spin assignments

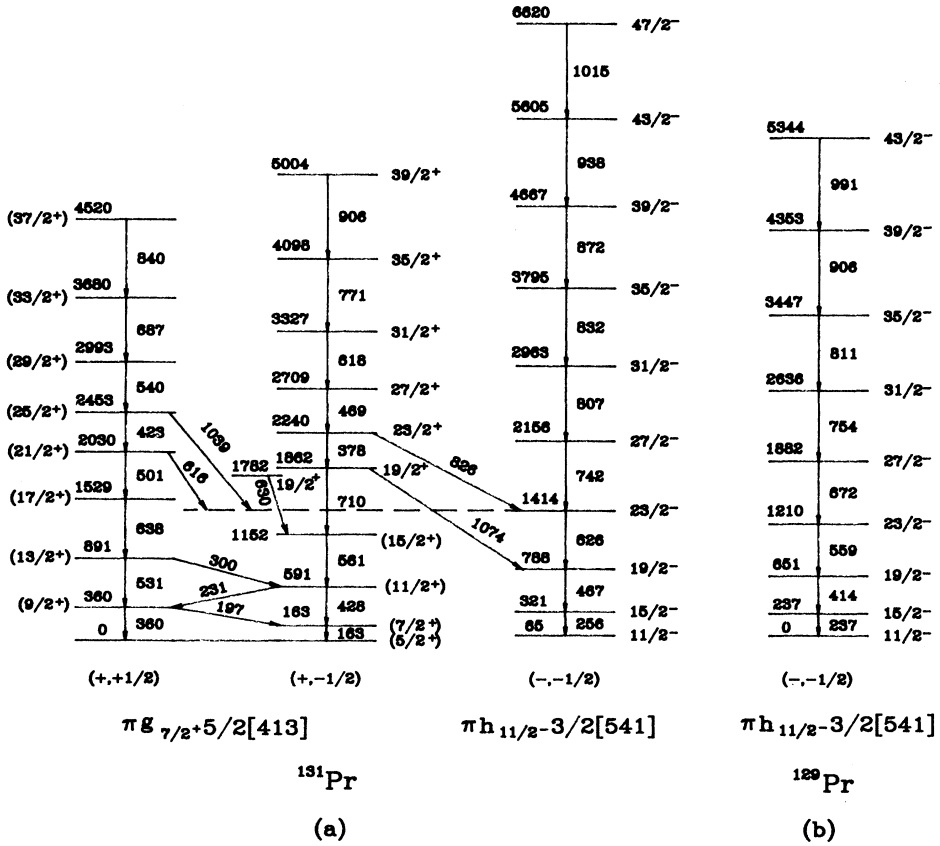

FIG. 1. Proposed level schemes for (a) ^{131}Pr and (b) ^{129}Pr. All energies are given in keV.

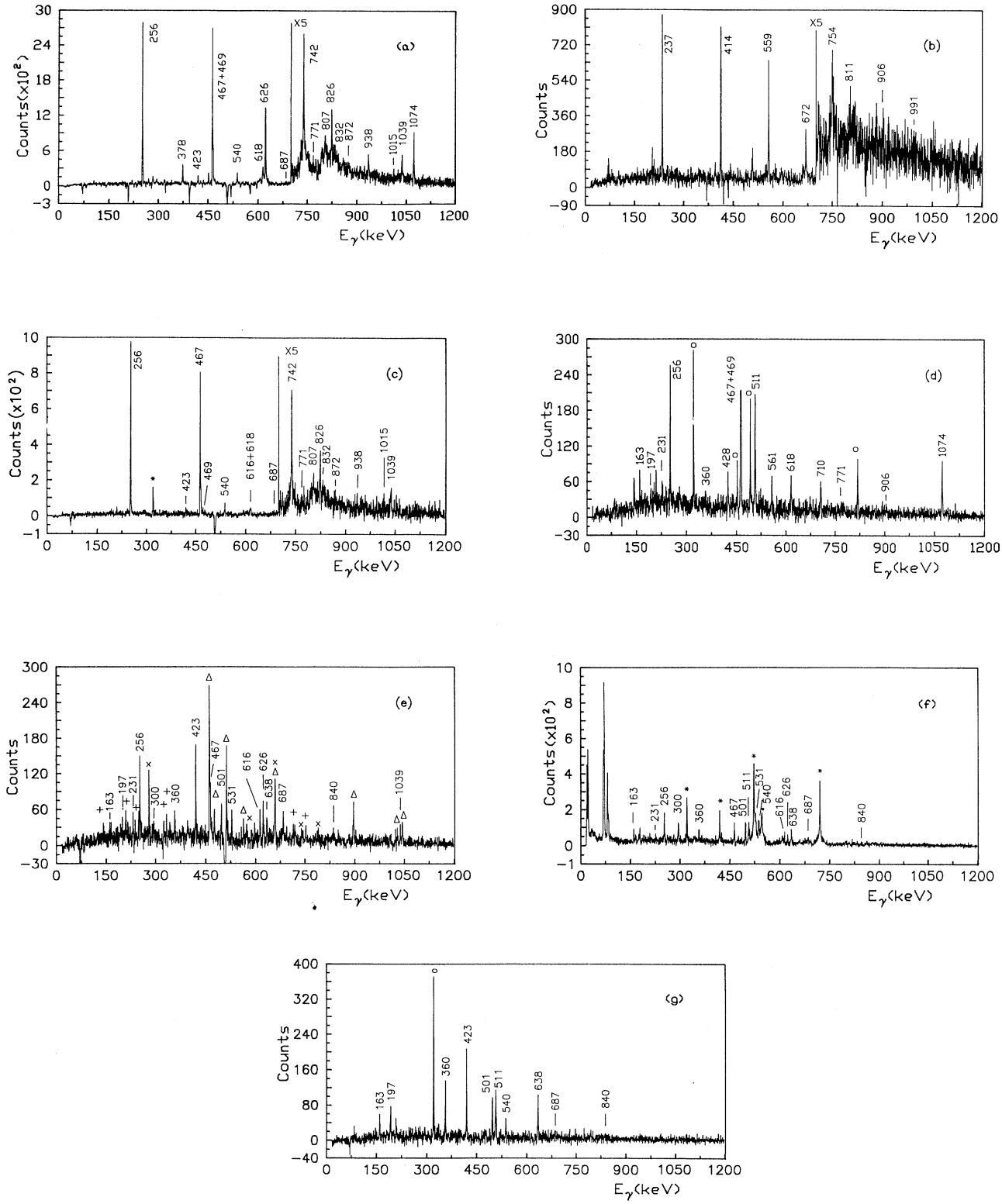

FIG. 2. Coincidence spectra: (a) The sum of spectra gated on the 256, 467, and 626 keV transitions in yrast band of ^{131}Pr. (b) The sum of spectra gated on the 237, 414, 559, and 672 keV transitions in yrast band of ^{129}Pr. (c), (d), (e), (f), and (g) The spectra gated on the 626, 378, 540, 423, and 531 keV transition individually. All energies are given in keV. ○, contamination from the ^{132}Pr β^+ + EC (electron capture) decay transitions. *, contamination from ^{107}Ag Coulomb excitation transitions. △, contamination from ^{132}La β^+ + EC decay transitions. ×, contamination from ^{132}Pr transitions. +, contamination from ^{129}Ce transitions.

TABLE I. γ energy, relative intensities, coefficients of angular distribution, spin, and parity of levels assigned to ^{129,131}Pr.

Isotope	E_γ (keV)	Intensity I_γ	A_{22}	A_{44}	Multipolarity	I_i^π	I_f^π
^{131}Pr	163	14.8(3.0)	0.04(3)	−0.09(4)	$M1$	$\frac{7}{2}^-$	$\frac{5}{2}^-$
	256	100(2.5)	0.28(3)	−0.15(4)	$E2$	$\frac{15}{2}^-$	$\frac{11}{2}^-$
	467	88.8(3.5)	0.29(2)	−0.13(5)	$E2$	$\frac{19}{2}^-$	$\frac{15}{2}^-$
	469	17.8(3.5)	0.35(5)	−0.09(3)	$E2$	$\frac{27}{2}^-$	$\frac{23}{2}^-$
	626	79.9(4.4)	0.41(3)	−0.15(7)	$E2$	$\frac{23}{2}^-$	$\frac{19}{2}^-$
	742	27.6(3.8)	0.09(10)	−0.17(5)	$E2$	$\frac{27}{2}^-$	$\frac{23}{2}^-$
	826	11.8(1.8)	−0.12(3)	−0.09(5)	$E1$	$\frac{23}{2}^+$	$\frac{23}{2}^-$
	1074	8.9(1.3)	−0.24(3)	0.01(4)	$E1$	$\frac{19}{2}^+$	$\frac{19}{2}^-$
	378	12.9(1.0)					
	618	16.0(2.6)					
	1039	6.8(1.0)					
	423	11.4(1.8)					
	540	10.7(2.0)					
^{129}Pr	237	67.8(2.2)	0.51(10)	−0.18(14)	$E2$	$\frac{15}{2}^-$	$\frac{11}{2}^-$
	414	100(2)	0.45(7)	−0.09(10)	$E2$	$\frac{19}{2}^-$	$\frac{15}{2}^-$
	559	79.7(2.8)	0.34(7)	−0.06(10)	$E2$	$\frac{23}{2}^-$	$\frac{19}{2}^+$
	672	36.5(1.2)					
	754	15.9(9)					

for the highest members in the bands are made under the assumption that the rotational band structures continue to high spin. The tentative spins and parities are shown in brackets. The relative intensities of the transitions in ^{131}Pr and ^{129}Pr were obtained from γ single spectra and from the angular distribution data.

The level schemes of ^{131}Pr and ^{129}Pr are mainly derived from the γ-γ coincidences. The coincidence spectrum obtained from the sum of spectra gated on the 256, 467, and 626 keV transitions in the yrast band of ^{131}Pr is shown in Fig. 2(a). The coincidence spectrum obtained from the sum of spectra gated on the 237, 414, 559, and 672 keV transitions in the yrast band of ^{129}Pr is presented in Fig. 2(b). The coincidence spectrum gated on the single 626 keV transition is given in Fig. 2(c). The 256, 467, 626, 742, 807, 832, 872, 938, and 1015 keV γ transitions in the yrast band of ^{131}Pr are observed in the spectra. The weaker transitions at 378, 469, 618, 771, 423, 540, and 687 keV in the sidebands which decay through 826, 1074 and 616, 1039 keV transitions to the yrast band, are also seen in these figures.

Two positive-parity rotational bands are observed in ^{131}Pr with $(\pi,\alpha)=(+,\pm\frac{1}{2})$ and shown to decay to the same level of the ground state band. The coincidence spectra gated on the 378, 540, 423, and 531 keV transitions are shown in Figs. 2(d), 2(e), 2(f), and 2(g), respectively. The 378 keV transition is in coincidence with the 163, 197, 231, 360, 428, 469, 618, 710, 771, and 906 keV transitions placed within the $(+,\pm\frac{1}{2})$ band structure. It is, however, also in coincidence with the 256 and 467 keV γ rays in the yrast band through a 1074 keV linking transition. The 423 keV transition is similarly in coincidence with the 163, 197, 231, 300, 360, 531, 638, 501, 540, 687, and 840 keV transitions in the $(+,\pm\frac{1}{2})$ band structure. It is also linked through the 616 keV transition to the 256, 467, and 626 keV γ rays in the yrast band. The 540 keV transition has the same coincidence relation as the 423 keV γ ray, but is linked via both the 1039 and the 616 keV transitions to the yrast band.

The γ transition intensities in the unfavored $(+,+\frac{1}{2})$

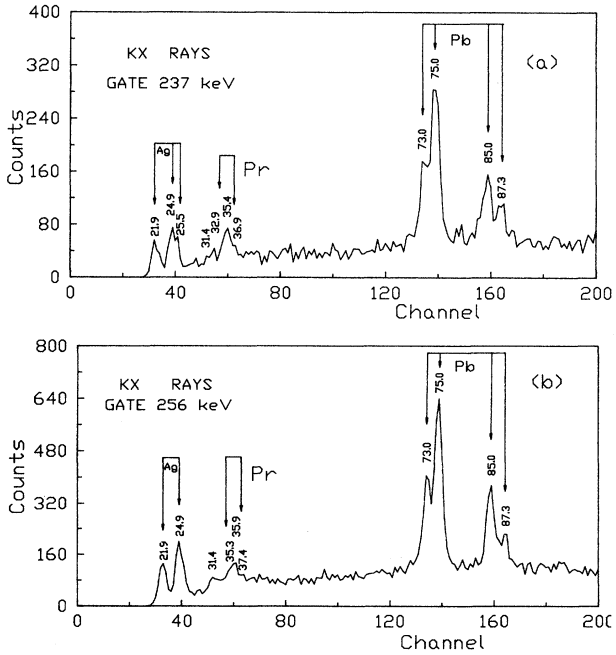

FIG. 3. The low energy part of the coincidence spectra: (a) gated on the 237 keV transition, (b) gated on the 256 keV transition. All energies are given in keV.

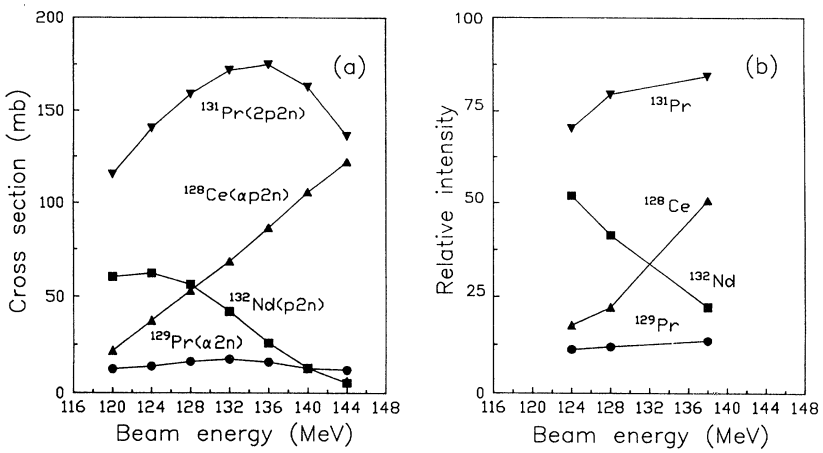

FIG. 4 (a) Excitation functions calculated by using the CASCADE code for ^{107}Ag(^{28}Si,x) reactions. (b) Excitation functions measured for selected transitions in the ^{128}Ce(206 keV, $2^+ \rightarrow 0^+$), ^{132}Nd(213 keV, $2^+ \rightarrow 0^+$), ^{131}Pr(256 keV, $2^+ \rightarrow 0^+$), and ^{129}Pr(237 keV, $2^+ \rightarrow 0^+$).

band are weaker than those in the favored $(+,-\frac{1}{2})$ band.

From the systematics in odd Pr nuclei, the yrast bands of ^{131}Pr and ^{129}Pr are based on the signature $\alpha=-\frac{1}{2}$ component of the $h_{11/2}\frac{3}{2}^-[541]$ configuration. The intense transitions of 256, 467, 626, and 742 keV are interpreted as forming a cascade of stretched $E2$ transitions in the low spin part of the yrast negative-parity band of ^{131}Pr. With $Z=59$ and assuming a prolate deformation $\varepsilon=0.20-0.25$ for ^{131}Pr, the available Nilsson orbitals are $\frac{3}{2}^+[411]$, $\frac{5}{2}^+[413]$, and the $\frac{3}{2}^-[541]$ intruder. The obvious choice for the tentative assignment of the $I=\frac{5}{2}$ ground state is then the $\frac{5}{2}^+[413]$ state based on a $g_{7/2}$ proton, and the two positive-parity bands are the two bands with opposite signature $(+,+)$ and $(+,-)$ based on this state.

There was little knowledge on the ^{129}Pr nucleus prior to the present work. It is a by-product of our experiment. There are three reasons to assign the band given in Fig. 1(b) to ^{129}Pr: (1) The γ-γ coincidence spectra gated on the 237 and 256 keV γ transitions (shown in Fig. 3) respectively show a similar K x-ray spectrum, which means that these γ transitions belong to Pr isotopes. Four Pr isotopes from ^{129}Pr to ^{132}Pr can be produced in ^{107}Ag(^{28}Si,x) reaction. The main γ-ray transitions in ^{130}Pr [10], ^{131}Pr, and ^{132}Pr [11] are known and none of the γ rays of Fig. 1(b) has been reported in these nuclei. (2) We have measured the experimental excitation function for the ^{107}Ag(^{28}Si,x) reactions and compared the exhibited trends for the ^{128}Ce, ^{132}Nd, ^{131}Pr, and ^{129}Pr nuclei (shown in Fig. 4) with the CASCADE calculations. The curve trend of the proposed ^{129}Pr transition agrees with the prediction from the CASCADE calculation. (3) The level structure of the yrast band fits very well in the systematics of Pr isotopes.

IV. DISCUSSION

In odd-proton Pr nuclei, the yrast band is based on the $\frac{11}{2}^-$ state . The level energy in the $\frac{11}{2}^-$ yrast state of ^{131}Pr is 65 keV higher than the $\frac{5}{2}^+$ ground state (Fig. 1). The systematics of the low spin part of these bands in several Pr isotopes is shown in Fig. 5. The dots represent the level spacing in the even-even Ce cores which have one proton less than the corresponding odd Pr isotopes. As can be seen, the spacings in the yrast bands of the Pr isotopes follow closely those of the cores. This is suggestive of a rotationally aligned particle, in this case an $h_{11/2}$ proton, coupled to the appropriate Ce core. The decrease in level spacing with decreasing neutron number indicates that the deformation of the nucleus is increasing, while the nucleus is further away from the $N=82$ shell closure. As a consequence, the energy of the $\frac{11}{2}^-$ state drops and approaches the ground state.

In order to elaborate on the detailed structure of the bands, the experimentally observed quantities are transformed to the rotating frame following the methods of Bengtsson and Frauendorf [12]. The angular momentum alignment i_x is given by the formula

$$i_x = I_x(\omega) - I_{x,\mathrm{ref}}(\omega) , \tag{2}$$

$$\omega = [E(I+1)-E(I-1)]/[I_x(I+1)-I_x(I-1)] , \tag{3}$$

the Routhian (the excitation energy in the rotating frame) $e'(\omega)$ is given by the formula

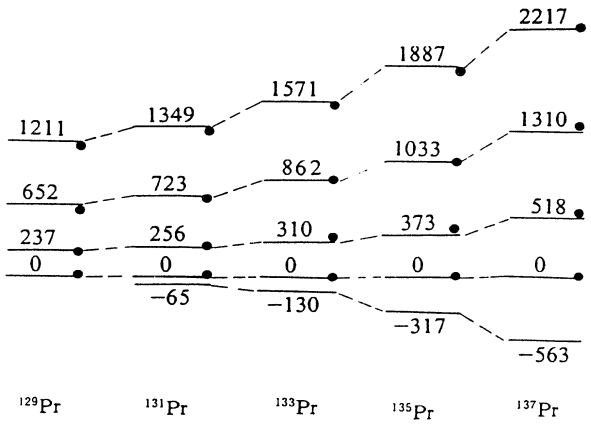

FIG. 5. The systematics of $\Delta I=2$ bands built on the $\frac{11}{2}^-$ states in the odd mass $^{129-137}$Pr isotopes. The energy of the $\frac{11}{2}^-$ states is set to zero and used as a reference. The filled circles represent the ground state band in the corresponding $^{A-1}$Ce core.

$$e'(\omega)=E'(\omega)-E'_{\rm ref}(\omega)\ . \tag{4}$$

Here, I_x is the total angular momentum component on the rotational axis given by

$$I_x=[(I+\tfrac{1}{2})^2-K^2]^{1/2}\ , \tag{5}$$

and $I_{x,\rm ref}$ is a reference based on a frequency-dependent moment of inertia, i.e.,

$$I_{x,\rm ref}(\omega)=\omega J_{\rm ref}=\omega(J_0+\omega^2 J_1)\ , \tag{6}$$

where J_0 and J_1 are the Harris parameters. The results of i_x and e' as a function of $\hbar\omega$ for ^{129,131}Pr are presented in Fig. 6. The values $J_0=17.0$ MeV$^{-1}\hbar^2$, $J_1=25.8$ MeV$^{-3}\hbar^4$ for ^{131}Pr and $J_0=18.8$ MeV$^{-1}\hbar^2$, $J_1=23.7$ MeV$^{-3}\hbar^4$ for ^{129}Pr were obtained from a fit to the yrast band in ^{130}Ce [4] and ^{128}Ce [13] above the first backbend, where the nuclear shape is expected to be more stable than in the ground state band.

In order to compare the experimental results with theoretical predictions, cranking shell model (CSM) calculations have been performed for ^{131}Pr and ^{129}Pr, as shown in Fig. 7. The deformation parameters used in the calculations are $\varepsilon_2=0.24$, $\varepsilon_4=0.0$, and $\gamma=0.0$ for ^{131}Pr, and $\varepsilon_2=0.26$, $\varepsilon_4=0.0$, and $\gamma=0.0$ for ^{129}Pr. The quadrupole deformations have been extracted from the 2^+ excitation energies in ^{130}Ce and ^{128}Ce, respectively [4,13,14]. The pairing gaps were set to $\Delta_p=1.10$ MeV for ^{131}Pr and $\Delta_p=1.05$ MeV for ^{129}Pr. These values were deduced from the odd-even mass differences. The proton Fermi energies λ_p of ^{131}Pr and ^{129}Pr have been chosen to reproduce the particle numbers $Z=59$ and $N=72$ and 70, respectively. In Fig. 7, the lowest energy single quasiproton states of negative parity are labeled by A, B, C, and D, and those of positive parity are labeled by E, F, ... The yrast band of ^{131}Pr and ^{129}Pr has a near constant alignment $i_x\approx 4.5\hbar$ and $5.0\hbar$, respectively, for $\hbar\omega<0.35$ MeV (Fig. 6). This is consistent with a band based on the decoupled $h_{11/2}$ proton as shown by the slope of level A (Fig. 7). In the yrast band of ^{131}Pr and ^{129}Pr, the $h_{11/2}$ proton blocks the first proton alignment, and, as a result, no backbend is observed in this band at low spin. The observed crossing frequency $\hbar\omega_c=0.39$ MeV for ^{131}Pr and 0.37 MeV for ^{129}Pr is only present in the negative-parity band, showing that this band crossing is most probably due to the second and third $h_{11/2}$ proton band crossing (BC) alignment. A similar upbend has been observed in the decoupled $h_{11/2}$ proton bands in ^{133}Pr [6] and ^{135}Pr [7]. The systematic comparison between experimental data and theoretical calculations of the BC crossing frequency $\hbar\omega_{\rm BC}$ in a series of Pr isotopes is given in Table II.

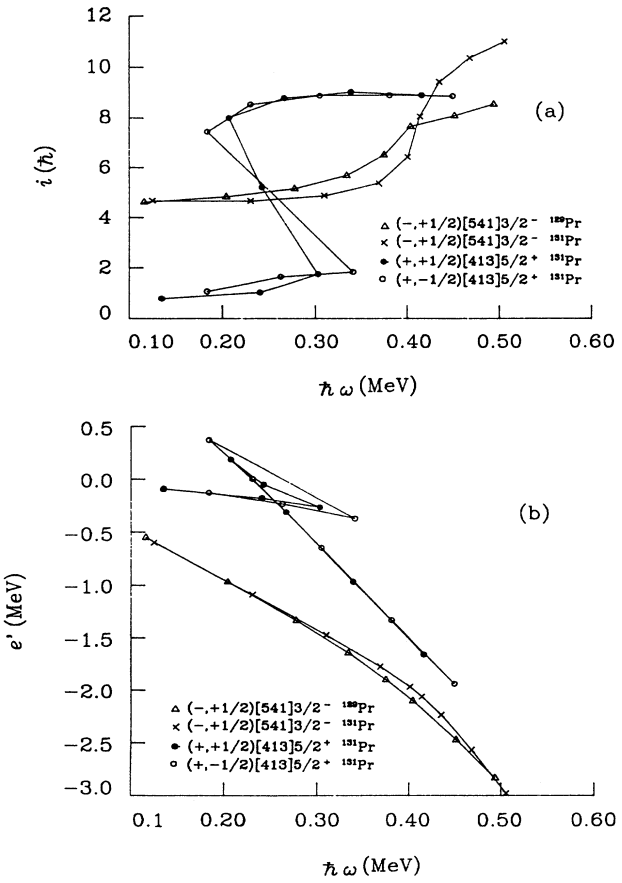

FIG. 6. The experimental alignment i_x (a) and Routhians e' (b) plotted versus the rotational frequency $\hbar\omega$ for the bands in ^{129,131}Pr. (X—yrast band of ^{131}Pr. △—yrast band of ^{129}Pr, ○—$\alpha=-\frac{1}{2}$ side band of ^{131}Pr, ●—$\alpha=+\frac{1}{2}$ side band of ^{131}Pr).

As shown in Table II, the theoretical values of $\hbar\omega_{\rm BC}$ are larger than the experimental results, especially in the lower Pr nuclei. It can be shown that the pairing force in these nuclei should be reduced in the three quasiparticle band. For ^{129}Pr and ^{131}Pr, if Δ_p is reduced by about 20%, the theoretical value will coincide with the experimental results. On the other hand, the experimental values of $\hbar\omega_{\rm BC}$ decrease with decreasing Pr isotopes, which may reflect the varying occupation probability of different orbitals as deformation is increasing. This might result in a lower quasiparticle energy for the $h_{11/2}$ orbital.

The alignment i_x and Routhian e' in the sidebands of ^{131}Pr (Fig. 6) indicate that these two positive-parity bands have almost identical behavior as would be expected from two bands of opposite signature based on the same configuration. At low spin, they have small alignment $i_x=1.5\hbar$ and small signature splitting. These properties are typical for a strongly coupled particle like the $g_{7/2}$ $\frac{5}{2}^+[413]$ proton. These bands exhibit a crossing at

TABLE II. Comparison of measured $\hbar\omega_{\rm BC}$ with the theoretical values in a series of Pr isotopes.

Isotope	$\hbar\omega_{\rm BC}$ (MeV) Exp.	Theory
^{129}Pr	0.37	0.44
^{131}Pr	0.39	0.45
^{133}Pr	0.43	0.46
^{135}Pr	0.46	0.47

$\hbar\omega_c = 0.25$ MeV above which the alignment stays rather constant at $i_x = 9.5\hbar$. The sharp backbend, the crossing frequency, and the gain in alignment $\Delta i_x = 8.0\hbar$ are similar to those that have been observed in the Ce [4,5] isotopes. The crossing is then interpreted as the alignment of a $h_{11/2}$ proton pair. The observed crossing frequency is somewhat lower than that of the CSM calculation $\hbar\omega_{AB} = 0.28$. The observed values of $\hbar\omega_{AB}$ in the two positive-parity bands are much lower than that of the ^{130}Ce core nucleus [4] where the first crossing is observed at $\hbar\omega_{AB} = 0.32$ MeV. One reason for this difference in frequency comes from the reduction in the proton pairing strength caused by the odd proton in the ^{131}Pr nucleus. Another possible reason for this difference in frequency could come from the possibility that the band of ^{130}Ce is γ soft and changes its shape easily. The ground state band can then gain in energy by adopting a triaxial shape and in this way increase the crossing frequency. The case is very similar to that seen in the ^{132}Ce core nucleus [5]. The systematic experimental values and the theoretical calculations of $\hbar\omega_{AB}$ in a series of Pr [6,7] and Ce [4,5] isotopes are given in Table III.

As mentioned in the Introduction, nuclei in this region are γ soft. Changes in the signature splitting are known to be strongly dependent on the γ deformation. Figure 8 shows that the calculated quasiparticle energies vary with different triaxial deformation for a fixed rotational frequency $\hbar\omega_c = 0.25$ MeV. The Fermi level for protons in

TABLE III. Comparison of measured $\hbar\omega_{AB}$ with the theoretical values in a series of Pr and Ce isotopes.

Isotope	$\hbar\omega_{AB}$ (MeV) Exp.	Theory
^{131}Pr	0.26	0.28
^{133}Pr	0.27	0.29
^{135}Pr	0.32	0.31
^{130}Ce	0.32	0.32
^{132}Ce	0.34	0.34

^{131}Pr lies near the bottom of the $h_{11/2}$ shell. The $h_{11/2}$ proton orbitals A and B have their minima at $\gamma \approx -10°$ and $\gamma > 0°$, respectively. When A and B are occupied, they tend to drive the nuclear shape towards $\gamma \geq 0°$. The positive-parity orbitals E and F are rather flat; therefore, the driving forces for the γ deformation are small in this case. In the bands seen here the observed signature splitting has essentially disappeared after the backbending in the $\frac{5}{2}^+[413]$ band. This shows that γ tends toward about 0°. The only other way the experimental signature splitting could be very small would be at $\gamma = -70°$, but with such a deformation the neutrons would not align at sufficiently low frequency to account for the first backbend. The systematics of signature splitting after the backbend in the $\frac{5}{2}^+[413]$ band of some Pr isotopes is as follows: ^{131}Pr, almost no signature splitting, while small

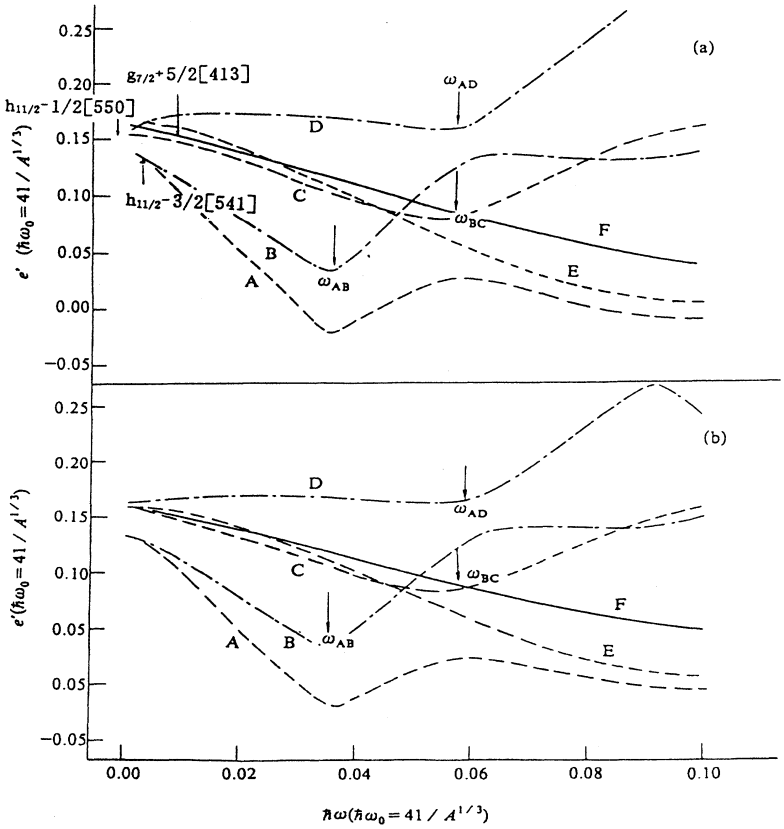

FIG. 7. Cranked shell model calculations of the quasiparticle energies for protons (a) ^{131}Pr and (b) ^{129}Pr. The Nilsson configurations are shown at $\hbar\omega = 0.0$. The various parity (π) and signature (α) combinations are $(\pi,\alpha) = (-,-\frac{1}{2})$, dashed; $(-,+\frac{1}{2})$, dot-dashed; $(+,+\frac{1}{2})$, solid; $(+,-\frac{1}{2})$, dotted.

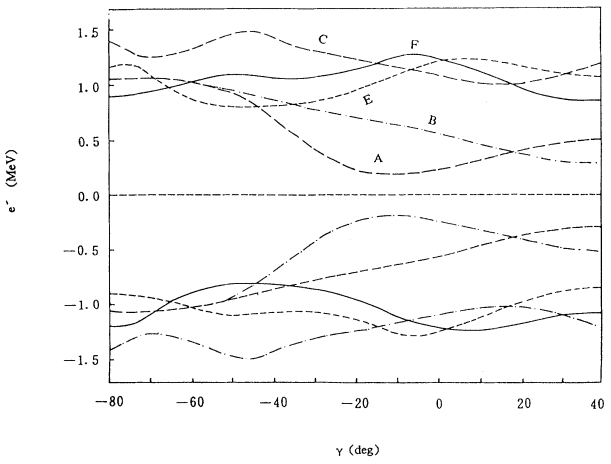

FIG. 8. Theoretical Routhians e' for the protons plotted versus γ at fixed $\hbar\omega=0.25$ MeV in ^{131}Pr. The Routhian assignments A, B, C, D, E, and F are the same as in Fig. 7.

signature splitting is present in ^{133}Pr and signature splitting and inversion occurs in ^{135}Pr.

V. CONCLUSIONS

In summary, the ^{129,131}Pr nuclei have been studied to high spin. The yrast band of ^{129}Pr based on a decoupled $h_{11/2}$ proton was found to have a band crossing at $\hbar\omega_c=0.37$ MeV, which is 0.07 MeV lower than that calculated by CSM. The difference between the experimental and theoretical crossing frequencies may indicate reduced pairing in this three quasiparticle band. Two positive-parity sidebands of ^{131}Pr based on the $g_{7/2}$ $\frac{5}{2}^+[413]$ proton configuration were also observed. The band crossing at $\hbar\omega_c=0.26$ MeV with a gain in alignment about $8\hbar$ was attributed to the alignment of two $h_{11/2}$ protons. The crossing frequency is about 20% lower than that observed in the ^{130}Ce core nucleus. This could be due either to the ^{130}Ce core being γ soft in its ground state band or to a reduction of the proton pairing strength in ^{131}Pr. The experimental observation that there is almost no signature splitting after the backbend in $g_{7/2}$ $\frac{5}{2}^-[413]$ band implies that the γ deformation moves toward 0° at the highest spin.

ACKNOWLEDGMENTS

This work was supported by the National Natural Science Foundation of China. The authors are grateful to Professor Y. S. Chen for valuable discussions. We are also acknowledging all staff members of the Tanden Accelerator Laboratory for providing the beam.

[1] G. A. Leander, S. Frauendorf, and F. R. May, in *Proceedings of the Conference on High Angular Momentum Properties of Nuclei,* Oak Ridge, 1982, edited by N. R. Johnson (Harwood, New York, 1983), p. 281.

[2] G. Anderson, S. E. Larron, G. Leader, P. Moller, S. G. Nilsson, I. Ragnasson, S. Aberg, R. Bengtsson, J. Dudek, B. Nerlo-Pomerska, K. Pomorski, and Z. Szymanski, Nucl. Phys. **A268**, 205 (1976).

[3] J. Nolan, D. M. Todd, P. J. Smith, D. J. G. Love, P. J. Twin, O. Andersen, J. D. Garrett, G. B. Hagemann, and B. Herskind, Phys. Lett. **108B**, 269 (1982).

[4] D. M. Todd, R. Aryaeinjad, D. J. G. Love, A. H. Nelson, P. J. Nolan, P. J. Smith, and P. J. Twin, J. Phys. G **10**, 1407 (1984).

[5] P. J. Nolan, A. Kirwan, D. J. G. Love, A. H. Nelson, D. J. Unwin, and P. J. Twin, J. Phys. G **11**, L17 (1985).

[6] L. Hildingsson, C. W. Beausang, D. B. Fossan, and W. F. Piel, Phys. Rev. C **37**, 985 (1988).

[7] T. M. Semkow, D. G. Sarantites, K. Honkanen, V. Abenanto, L. A. Adler, C. Baktash, N. R. Johnson, I. Y. Lee, M. Oshima, Y. Schutz, Y. S. Chen, J. X. Saladin, C. Y. Chen, O. Dietzsch, A. J. Larabee, L. L. Riedinger, and H. C. Griffin, Phys. Rev. C **34**, 523 (1986).

[8] M. J. Godfrey, P. J. Bishop, A. Kirman, P. J. Nolan, D. J. Thornley, D. J. Unwin, D. J. G. Love, and A. H. Nelson, J. Phys. G **13**, 1165 (1987).

[9] Guo Yingxiang, Sun Xiangfu, Luo Yixiao, Lei Xiangguo, Xu Xiaoji, Wen Shuxian, Li Shenggang, Weng Peikun, and Yan Chunxiang, Nucl. Electron. Detect. Tech. **11**, 6 (1991).

[10] R. Ma, E. S. Paul, S. Shi, C. W. Beauang, W. F. Piel, Jr., N. Xu, and D. B. Fossan, Phys. Rev. C **37**, 1926 (1988).

[11] S. Shi, C. W. Beausang, D. B. Fossan, R. Ma, E. S. Paul, and N. Xu, Phys. Rev. C **37**, 1478 (1988).

[12] R. Bengtsson and S. Frauendorf, Nucl. Phys. **A327**, 139 (1979); **A314**, 27 (1979).

[13] J. C. Wells, N. R. Johnson, J. Hattula, M. P. Fewell, D. R. Haenni, I. Y. Lee, F. K. McGowan, J. W. Johnson, and L. L. Riedinger, Phys. Rev. C **30**, 1532 (1984).

[14] L. Grodzins, Phys. Lett. **2**, 88 (1962).